Gravity wave breaking over the central Alps:

Role of complex topography

Qingfang Jiang, UCAR/NRL, Monterey, CA
James D. Doyle, Naval Research Laboratory, Monterey, CA

1. Introduction

Turbulent break-down of mountain waves has been the subject of numerous studies during the last three decades because of its potential threat to aircraft, its role in global momentum balance, and its connection to strong surface windstorms over mountain lee-slopes. While a great deal has been learned from idealized numerical studies, direct observations of mountain wave breaking are still rare. Breaking gravity waves excited by complex terrain in the central Alps associated with a southerly foehn event were observed on 21 October, 1999 during the Mesoscale Alpine Programme (MAP) Special Observational Period (SOP, IOP 8). In this study, some mechanistic aspects of the wavebreaking event is investigated though observational data analysis, real data simulations, and idealized simulations.

2. Observations

On October 21, 1999, a shallow southerly foehn developed over the Alps associated with the approach of a deep cyclone from the west. A pressure ridge was located over the eastern Alps, which advected warm air from the south across the Alps. In the early morning, the National Center for Atmospheric Research (NCAR) Electra research aircraft equipped with flight level instruments, Global Positioning System (GPS) dropsondes, and downlooking Scanning Aerosol Backscatter Lidar (SABL) executed two transverses across the Ötztaler Alpen and the Inn valley at approximately the 5.7km level during a period of approximately 60min. to sample gravity waves (Fig. 1). Strong turbulence was encountered likely associated with mountain wavebreaking. Eleven GPS dropsondes were deployed with a relatively uniform spacing along the two transverses and SABL provided clear backscatter (Fig. 1). Figures 1 and 2 show vertical sections of wind and potential temperature created by manual analysis of the data from seven GPS dropsondes with the terrain beneath the first transverse. Strong flow descent over the lee-slope of Ötztaler Alpen, associated with a severe windstorm is evident. Further downstream a transition occurs associated with a hydraulic jump as indicated by sharp decrease of wind speed and ascent of isentropes. Between 47.5-47.7N, a super-adiabatic layer exists between 3-5km with local wind reversal and turbulence. The descent-ascent pattern matches well with the SABL backscatter. The vertical sections created using data from 7 dropsondes along the second transverse (not shown) indicate downstream propagation of the hydraulic jump.

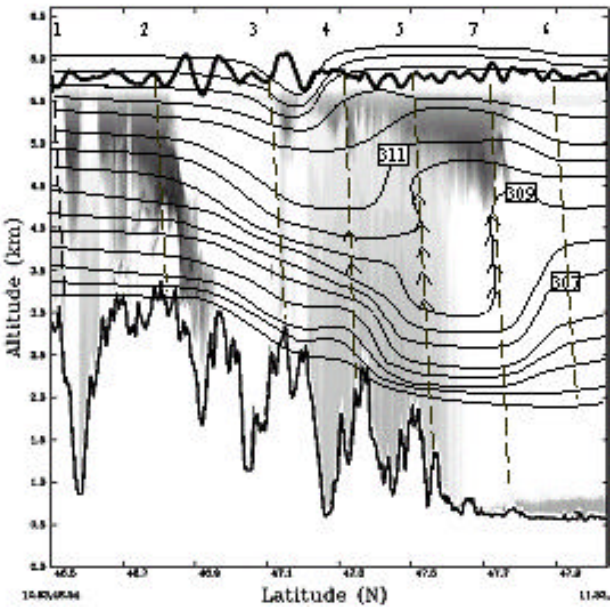

Figure 1. The SABL backscatter coefficient (in gray), vertical displacement (thick solid curve between 5-6km), and potential temperature contours (solid) along the first transverse. The vertical displacement is computed from flight level wind using equation (1). The potential temperature is derived from GPS dropsondes (see text for details). The dashed lines are GPS dropsonde trajectories and the dropsondes are numbered sequentially in time. The symbol ^ indicates turbulent regions above the boundary layer. The terrain along the flight track is shown at the bottom.

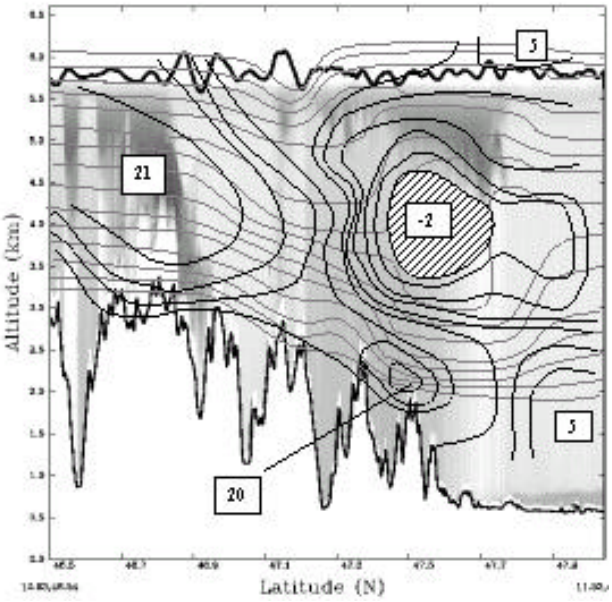

Figure 2. Same as Fig. 1 except with the isentropes in gray lines and along flight direction wind component in dark contours. The wind maxima and minima are labeled. Region with reversed wind is hatched.

The vertical displacement derived from the flight level wind components (following Smith et al, 2002) indicates the presence of both smooth waves and sharp-peaked breaking waves. The turbulent kinetic energy (TKE) and the buoyancy production rate of TKE computed from 1Hz data are plotted in Fig. 3. For the first transverse, TKE clusters are located between 46.9-47.4N and the contribution from v-component dominates. At the flight level, the air is convectively unstable between 46.9-47.4N as indicated by positive buoyancy production rate of TKE (Fig. 3). The second transverse observes three local TKE maxima and severe turbulence occurs around 47.5N. The turbulence is much more severe and more isentropic than observed along the first transverse. Along the second transverse, the buoyancy force consumes turbulence between 46.9-47.4N and produces turbulence near 47.5N, which is consistent with the hydraulic jump propagation suggested by the dropsonde analysis.

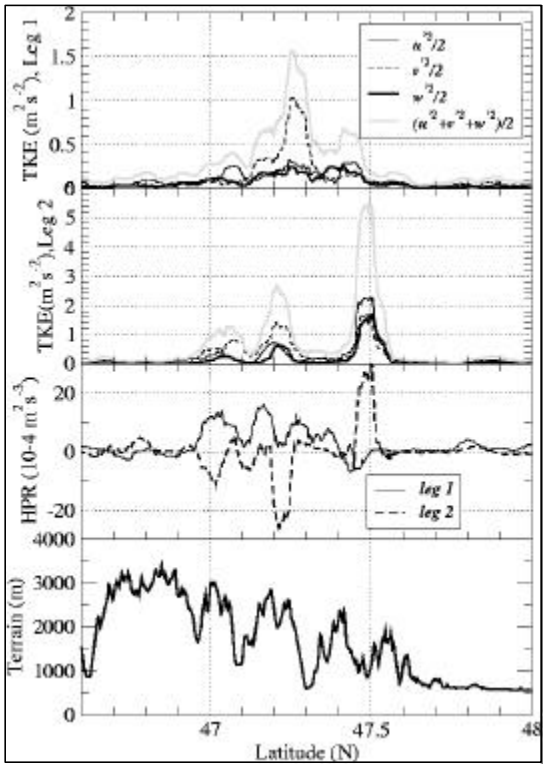

Figure 3. Turbulence kinetic energy (TKE) and the buoyancy production rate of TKE along the two transverses as a function of the latitude. Terrain along the first transverse is plotted for reference.

3.Wavebreaking over multiscale terrain

The multiscale nature of the terrain beneath the flight level is evident (Fig. 1). The terrain spectrum indicates three dominant scales, >85km, 35km, and 10km. Similarly, flight level velocity spectra show multiple energy-containing spikes, approximately corresponding to the dominant terrain scales. A number of idealized 2-D simulations have been performed with a smooth large scale terrain with smaller scale features superposed on the lee-slope. The simulations indicate that smaller scale terrain promotes wave breaking, significantly enhances downslope windstorm, and increases mountain drag (Jiang and Doyle 2003).

4.Conclusions

Breaking mountain waves over the central Alps observed during the MAP SOP is examined through the analysis of aircraft data, GPS dropondes, radiosondes, and airborne lidar images, and numerical modeling. The focus of this study is the role of multiscale terrain on mountain wavebreaking.

The occurrence of the wave-breaking on October 21, 1999, was associated with a mean state characterized by vertical wind (speed and directional) shear and a critical level with a southerly (cross-mountain) wind component that decreased to zero and a Richardson number less than unity just above the NCAR Electra flight level of 5700m, as indicated by a nearby radiosonde. The turbulence induced by wave breaking was reported by flight scientists. During the first transverse, the turbulent region was convectively unstable as indicated by the positive explicit heat flux.. The second transverse illustrated the evolution of turbulence and fluxes 30 min. after the first transverse. The flight level data for the second transverse indicated that the turbulence was much stronger and the TKE maximum advected downstream. The GPS dropsonde data was used to diagnose a hydraulic jump that

was located just below the flight level and was associated with strong down slope winds, a sudden transition to turbulence with a local wind reversal, and convective instability.

The strong down slope winds and hydraulic jump are captured by a real data 1-km COAMPS simulation. Some theoretical aspects of the wave breaking are examined based on the real data simulation and idealized 2-D simulations with multi-scale terrain. Shorter waves excited by smaller scale terrain superposed on the leading edge of the longer waves corresponding to large scale terrain promote wave breaking and significantly modify the horizontal and vertical distribution of TKE.

1. Acknowledgement

This research was supported by the Office of Naval Research (ONR) program element 0601153N. The data for the field program was collected in a joint effort by the MAP scientists. And staff, especially our colleagues in the gravity wave breaking team: Drs. A. Broad, D. Fritts, K. Hoinka, J. Kuettner, G. Poulos, R. B. Smith, S. Smith, and H. Volkert.

2. References

Jiang, Q., and J. D. Doyle, 2003: Gravity wave breaking over the central Alps: Role of complex terrain. *J. Atmos. Sci.*, submitted.

Smith, R. B., S. Skubis, J. D. Doyle, A. S. Broad, C. Kiemle, and H. Volkert, 2002: Mountain waves over Mont Blanc: Influence of a stagnant boundary layer. *J. Atmos. Sci*., **59**, 2073-2092.